# Mo $L_{III}$-edge XANES Study of Catalytically Active Mo Species on Silica–Alumina Supports for Methane Dehydroaromatization

Hirofumi Aritani,*[1] Satoru Shinohara,[1] Shin-ichi Koyama,[1] Kazuo Otsuki,[1] Takashi Kubo,[2] and Atsushi Nakahira[2]
[1]*Department of Applied Chemistry, Saitama Institute of Technology, Fukaya 369-0293*
[2]*Graduate School of Engineering, Osaka Prefecture University, Sakai, Osaka 599-8531*

(Received January 10, 2006; CL-060031; E-mail: hirofumi.aritani@nifty.com)

L-edge XANES spectroscopy is applied to characterize the active Mo species for methane dehydroaromatization over $MoO_3/SiO_2–Al_2O_3$ and $MoO_3$/H–MFI. For highly active $MoO_3$(7.5 wt %)/H–MFI in $Si/Al_2 = 90$, dispersed molybdenum(II) carbide species are formed with oxy-carbide species after the reaction. Partially reduced species ($Mo^{4+}$) are formed on amorphous $SiO_2–Al_2O_3$ support, as well as $MoO_3$/H–MFI in high $Si/Al_2$ ratio. In contrast, formation of deeply reduced ions such as metallic ones on H–MFI with low $Si/Al_2$ ratio also gives low activity. It is suggested that stable molybdenum(II) carbide can be formed dispersively on H–MFI ($Si/Al_2 = 90$) even in coexistence of oxo-species.

Molybdena-based catalysts were generally active for partial oxidation of alkenes, and the catalytic activity is based on redox performance of Mo ions in many cases.[1–3] Since Wang et al.[4] and Wang et al.[5] reported the methane dehydroaromatization over $MoO_3$/H–MFI catalysts in the absence of oxygen, many workers have focused on this catalyst system for an application of novel GTL process. Many workers have revealed that reduction of $Mo^{6+}$ ions proceeds in the initial reaction step, and then Mo ions react methane to form carbide species, $Mo_2C$, in the next step.[6–8] It is thus accepted that active Mo species consist of reduced ions, mainly $Mo^{2+}$, with molybdenum carbide and/or oxy-carbide species on H–MFI.[9] However, deactivation cannot be avoided by carbon deposition at the same time. As a responsible Mo species, $\alpha$-$Mo_2C$ (fcc), $\beta$-$Mo_2C$ (hcp), and/or oxy-carbide-type species[9–14] have been proposed. But detail of the active Mo species on both H–MFI and other silica–alumina supports has been unclear because characterization of reduced Mo ions ($Mo^{2+}$) is difficult. On the other hand, it is likely that the activity of methane conversion and its deactivation rate depend on the property of silica–alumina supports.[10,15–19] In fact, molybdena supported on amorphous silica–alumina also shows dehydroaromatization activity, while it is lower than that on H–MFI. Relation between the silica–alumina support (with surface acidity) and active Mo species formed in the reaction is thus important to clarify the formation process of highly active Mo. In this study, Mo $L_{III}$-edge XANES is applied to characterize the Mo species on H–MFI and silica–alumina supports. Because the XANES spectrum probes the orbitals of 4d character participating in Mo–C and/or Mo–O bonds, structural information reflects the spectrum sensitively even in reduced Mo ions.[20–22] By comparing a H–MFI supports with amorphous silica–alumina ones, reduction behavior of Mo ions can be provided.

Catalysts were prepared by impregnation of each silica–alumina support with aqueous ammonium heptamolybdate (AHM) solution and followed by drying overnight and calcination at 773 K for 3 h. Amount of $MoO_3$-loading is 7.5 wt % in all the samples. Amorphous $SiO_2–Al_2O_3$ (JRC-SAH-1, 28.6 wt % $Al_2O_3$; denoted as SAH-1) and H–MFI ($Si/Al_2 = 40$, synthesized; $Si/Al_2 = 90$, JRC-Z5-90H; $Si/Al_2 = 1880$, Tosoh HSZ-890HOA) supports were used. Mo $L_{III}$-edge XANES spectra were measured in BL1A of UVSOR-IMS in total-electron yield mode. Photon energy was calibrated by using Mo metal-foil at Mo $L_{III}$-edge, and normalized XANES spectra and their second derivatives are shown. Catalytic reaction was carried out in a fixed bed flow reactor. Each catalyst (0.250 g) was placed in a quartz-tube reactor, and pretreated in He flow (30 mL $min^{-1}$) at 973 K for 1 h. Then, $CH_4$ (10%)–He gas was fed to the reactor at 973 K. The total flow rate was 30 mL $min^{-1}$ ($SV = 7.2\,L\,g^{-1}\,h^{-1}$). The products were analyzed by two online GCs (Shimadzu GC-3BF and GC-4BT) equipped with VZ-7 and Gaskuropack-54 columns.

In brief, methane dehydroaromatization reactivity over $MoO_3$/SAH-1 and $MoO_3$/H–MFI are summarized as Table 1. $C_6H_6$ selectivity is almost 100% in all cases, indicating selective reactivity is shown. $MoO_3$/SAH-1 shows low activity while deactivation rate is very low. It possesses that active Mo species are formed even on amorphous $SiO_2–Al_2O_3$. For H–MFI supports, the activity depends on the $Si/Al_2$ ratio. $MoO_3$/H–MFI in $Si/Al_2 = 90$ shows the maximum activity (35.2% of benzene yield at 75 min). In this case, the yield kept 16.4% for 250 min. High ratio ($Si/Al_2 = 1880$) gives quite low activity.

Figure 1 shows the $L_{III}$-edge XANES spectra of reference Mo samples. It is clear that edge energy values of XANES spectra in $MoO_2$, $\alpha$-$Mo_2C$, and Mo metal are different from each other. To clarify the difference, the second derivatives of XANES spectra are also shown in Figure 1. Each minimized peak is due to a peak component of original XANES. The difference of energy value is significantly between $Mo_2C$ (at 2525.3 eV in a minimum peak due to absorption edge) and Mo metal (at 2524.7 eV). This assignment can be applied to characterize the reduced Mo ions. As a reference, the spectrum of partially oxidized $Mo_2C$ (denoted as $Mo_2C$ (oxd.)), which is calcined at 473 K for 0.5 h, is also shown in Figure 1. $Mo_2C$ phase can be seen by XRD in the sample. The energy of a first minimum peak (at 2525.7 eV) is higher than that of bare $Mo_2C$ but lower than that of $MoO_2$. Because stable Mo oxy-carbide does not exist commercially, the $Mo_2C$ (oxd.) can be applied as a reference oxy-carbide sample.

Figure 2 shows the $L_{III}$-edge XANES spectra of $MoO_3$/SAH-1 and $MoO_3$/H–MFI ($Si/Al_2 = 90$) catalysts before/after the reaction. For $MoO_3$/SAH-1, it can be presumed that octahedral

**Table 1.** Catalytic activity for methane dehydroaromatization at 973 K

| Catalyst | Maximum activity | | For 360 min |
|---|---|---|---|
| | $C_6H_6$ Yield/% | (Time/min) | $C_6H_6$ Yield/% |
| $MoO_3$/SAH-1 | 6.0 | (145) | 5.5 |
| $MoO_3$/H–MFI | | | |
| $Si/Al_2 = 40$ | 29.9 | (40) | 8.1 |
| $Si/Al_2 = 90$ | 35.2 | (75) | 16.4 |
| $Si/Al_2 = 1880$ | 10.2 | (40) | 0.0 |

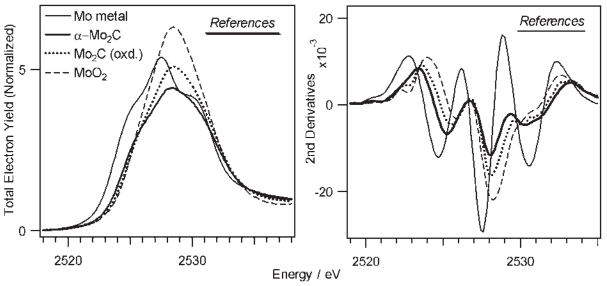

**Figure 1.** Mo $L_{III}$-edge XANES spectra (left) and their second derivatives (right) of reference compounds: $MoO_2$, $Mo_2C$, partially oxidized $Mo_2C$, and Mo metal.

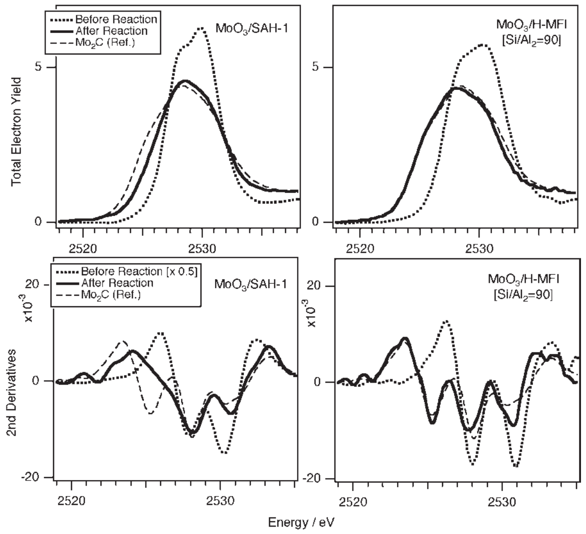

**Figure 2.** Mo $L_{III}$-edge XANES [top] and their second derivatives [bottom] of $MoO_3$/SAH-1 and $MoO_3$/H–MFI ($Si/Al_2 = 90$) before/after dehydroaromatization of methane at 973 K.

$Mo^{6+}$ ions are changed definitely to form reduced species, which has some differences from $Mo_2C$, by the reaction. $Mo^{6+}$-species on H–MFI (90) are also reduced by the reaction, but the spectrum after the reaction is similar to that of $Mo_2C$. It is summarized that reductive effect of Mo species on H–MFI (90) by the reaction is larger than that on SAH-1, and the difference relates to the catalytic activity. To clarify the differences, the second derivatives of their spectra can be evaluated. For $MoO_3$/SAH-1, only shoulder peak at ca. 2525 eV can be seen, and another components of reduced ions seem to be overlapped at 2528 eV (maybe due to $Mo^{4+}$ species) with remained $Mo^{6+}$ ions. These results suggest that partially reduced species (without deep reduction to form $Mo^{2+}$ ions) are brought about by the reaction. On the other hand, the components in $MoO_3$/H–MFI (90) after the reaction are quite similar to those of $Mo_2C$, indicating the formation of molybdenum(II) carbide species in major. By XRD analysis, $Mo_2C$ phase can slightly be seen with a very low intensity, and thus, most of Mo species are well dispersed. At the same time, MFI-phase in $MoO_3$/H–MFI is almost kept on after the reaction.

In Table 2 are summarized the results of the second derivatives of XANES, the results of $MoO_3$/H–MFI in $Si/Al_2 = 40$ and $Si/Al_2 = 1880$ after the reaction are also different from that in $Si/Al_2 = 90$. For $Si/Al_2 = 90$, slight difference can be seen in higher energy region (at 2531 eV) from $Mo_2C$ and partially oxidized one, suggesting the presence of oxidized ions such as $Mo^{6+}$ (in AHM) because a peak around 2524.7 eV (due to $Mo^0$) is absent. These results present the formation of Mo oxy-carbide species on $MoO_3$/H–MFI (90), and the species can act as the highly active species for dehydroaromatization. It can also be presented that reacted $MoO_3$/H–MFI in both $Si/Al_2 = 40$ and $Si/Al_2 = 1880$ shows less formation of $Mo_2C$-like species. In case of $Si/Al_2 = 40$, other component (peak at 2524.7 eV) due to metallic-like reduced ions can slightly be seen, indicating the formation of deeply reduced ions. In contrast, $Mo^{6+}$ species remains dominantly in $Si/Al_2 = 1880$. The relation between reducibility of Mo ions and $Si/Al_2$ ratio of H–MFI is very important, and low $Si/Al_2$ ratio tends to bring about reduction of Mo ions deeply. It is concluded that formation of dispersed molybdenum(II) carbide species with oxo species is a key role for generation of active species. Reduced state of Mo-carbide species is very important; low activity brings about the formation of deeply reduced ions such as metallic ones. It is suggested that stable molybdenum(II) carbide on H–MFI (90) can be formed even in coexistence of oxo species. Structural information of Mo species can directly be given by L-edge XANES study, as described above.

**Table 2.** Peak components obtained by second derivatives of XANES

| Catalyst | Energy of the peaks / eV | | |
|---|---|---|---|
| Mo metal | 2524.7 | 2527.6 | 2530.6 |
| $Mo_2C$ (α-) | 2525.3 | 2528.0 | (2530.2)[a] |
| $Mo_2C$ (oxd.) | 2525.7 | 2528.0 | (2530.1)[a] |
| $MoO_2$ | 2525.8 | 2528.2 | |
| $(NH_4)_6Mo_7O_{24}\cdot 4H_2O$ | | 2527.6 | 2530.8 |
| $MoO_3$/SAH-1 [after reaction] | | 2527.8 | 2530.1 |
| $MoO_3$/H–MFI [after reaction] | | | |
| $Si/Al_2 = 40$ | (2524.7)[a] | 2527.6 | 2530.6 |
| $Si/Al_2 = 90$ | 2525.8 | 2527.7 | 2530.7 |
| $Si/Al_2 = 1880$ | | 2527.8 | 2530.8 |

[a] Small intensity.

The XANES measurements were supported by the Joint Studies Program (Proposal No. 16-501 and others) of UVSOR in Institute for Molecular Science (IMS), Japan. This work was supported by Iketani Science and Technology Foundation (No. 0151019).

## References

1 J. Engelhardt, J. Goldwasser, W. K. Hall, *J. Catal.* **1982**, *76*, 48.
2 B. N. Shelimov, I. V. Elev, V. B. Kazansky, *J. Catal.* **1986**, *98*, 70.
3 K. Tanaka, K. Miyahara, K. Tanaka, *J. Mol. Catal.* **1982**, *15*, 133.
4 D. Wang, J. H. Lunsford, M. P. Rosynek, *J. Catal.* **1997**, *169*, 347.
5 L. Wang, Y. Xu, S.-T. Wong, W. Cui, X. Guo, *Appl. Catal., A* **1997**, *152*, 173.
6 P. Mériaudeau, L. V. Tiep, V. T. T. Ha, C. Naccache, G. Szabo, *J. Mol. Catal. A: Chem.* **1999**, *144*, 469.
7 P. Mériaudeau, V. T. T. Ha, L. V. Tiep, *Catal. Lett.* **2000**, *64*, 49.
8 D. Ma, Y. Shu, M. Cheng, Y. Xu, X. Bao, *J. Catal.* **2000**, *194*, 105.
9 S. Liu, L. Wang, R. Ohnishi, M. Ichikawa, *J. Catal.* **1999**, *181*, 175.
10 W. L. George, D. Meitzner, R. W. Borry III, E. Iglesia, *J. Catal.* **2000**, *191*, 373.
11 L. Chen, J. Lin, H. C. Zeng, K. L. Tan, *Catal. Commun.* **2001**, *2*, 201.
12 R. W. Borry, III, Y. H. Kim, A. Huffsmith, J. A. Reimer, E. Iglesia, *J. Phys. Chem. B* **1999**, *103*, 5787.
13 V. T. T. Ha, L. V. Tiep, P. Meriaudeau, C. Naccache, *J. Mol. Catal. A: Chem.* **2002**, *181*, 283.
14 H. Liu, W. Shen, X. Bao, Y. Xu, *Appl. Catal., A* **2005**, *295*, 79.
15 P. L. Tan, Y. L. Leung, S. Y. Lai, C. T. Au, *Catal. Lett.* **2002**, *78*, 251.
16 Y. Shu, D. Ma, L. Xu, Y. Xu, X. Bao, *Catal. Lett.* **2000**, *70*, 67.
17 Y. Shu, D. Ma, X. Bao, Y. Xu, *Catal. Lett.* **2000**, *66*, 161.
18 K. Chen, S. Xie, A. T. Bell, E. Iglesia, *J. Catal.* **2001**, *198*, 232.
19 C. Zhang, S. Li, Y. Yuan, W. Zhang, T. Wu, L. Lin, *Catal. Lett.* **1998**, *56*, 207.
20 J. Evans, W. Frederick, W. Mosselmans, *J. Phys. Chem.* **1991**, *95*, 9673.
21 H. Aritani, T. Tanaka, T. Funabiki, S. Yoshida, K. Eda, N. Sotani, M. Kudo, S. Hasegawa, *J. Phys. Chem.* **1996**, *100*, 19495.
22 H. Aritani, O. Fukuda, A. Miyaji, S. Hasegawa, *Appl. Surf. Sci.* **2001**, *80*, 261.

Published on the web (Advance View) March 18, 2006; DOI 10.1246/cl.2006.416